ELSEVIER

Polymer 42 (2001) 6129–6140

polymer

www.elsevier.nl/locate/polymer

Comparison of polymer blends and copolymers by broadband dielectric analysis

Nobuhiro Miura[a,1], William J. MacKnight[a], Shiro Matsuoka[b], Frank E. Karasz[a,*]

[a]*Department of Polymer Science and Engineering, University of Massachusetts, Amherst, MA 01003-4530, USA*
[b]*Polymer Research Institute, Polytechnic University, Six Metrotech Center, Brooklyn, NY 11201, USA*

Received 18 August 2000; received in revised form 8 January 2001; accepted 8 January 2001

Abstract

Dielectric relaxation measurements on poly *o*-chlorostyrene (PoCS), polystyrene (PS), a 50 mol% PoCS/PS blend, and a 50 mol% P(oCS/S) random copolymer were made in the frequency range 1 mHz to 1 MHz as a function of temperature. The α-relaxation process associated with micro Brownian motion of the chain was observed in each sample. The shape of the absorption $\epsilon''(\omega)$ of the copolymer was nearly the same as that of PS and of PoCS, and was considerably narrower than that of the blend. The broadened relaxation curve of the blend relative to the copolymer was well explained by a convolution of the individual relaxation processes, which were obtained in the copolymer by assuming equivalence to an ideal homogeneous mixture of two segments. The distribution, $P(\log \tau)$, of the peak position was modeled by a Gaussian error function. To apply the Vogel–Fulcher equation, the distribution $P(T_0)$ of the Vogel–Fulcher temperature, T_0, was calculated from $P(\log \tau)$. To reflect the cooperative motion, T_0 was distributed between the T_0 of PoCS and that of PS. This is equivalent to assuming that the broadened loss peak in the blend is caused by localized concentration fluctuations on the scale of the segmental motion. The *g*-factor calculated from the relaxation strength of the polymer blend was nearly the same as that of PS and of PoCS, but was considerably smaller than that of the copolymer. This difference suggests that the local environment of the dipole moment of the chlorostyrene unit in the blend is similar to that of the homopolymer.

Keywords: Poly *o*-chlorostyrene; Polystyrene; Polymer blends

---

1. Introduction

The definition of miscibility generally satisfies the thermodynamic criteria for a single-phase system (see [1–4]). However, miscibility in polymer blends is a relative term, and depends on the scale of homogeneity. It also depends, therefore, on the measurement technique employed. For example, if only one T_g is detected by DSC, the sample of a mixture of two constituents may be deemed miscible [1–4]. However, it is possible to exhibit a minimum degree of homogeneity for both polymer blends and copolymers larger than the monomer unit scale.

One reason for the apparent technique dependence of miscibility is the qualitative difference between the static structure and the dynamical property measured. Observation by a static method in the mixture will give information about the composition of the blend, such as how the polymer constituents interpenetrate each other [5]. On the other hand, dynamical properties such as the spin–lattice relaxation time T_1 or spin–spin relaxation time T_2 in NMR [6,7], and the distribution of T_g [8] will yield information regarding the heterogeneity of molecular motions. The presence of a broad single T_g implies that the constituent polymers of the blend move together but the dynamics are not uniform. This cooperative motion is an important aspect of miscibility, but is not completely understood.

Dielectric relaxation analysis can contribute to the understanding of the cooperative motion, because it is concerned with the movement of dipoles [9,10]. In addition, because of the wide range of frequencies that can be covered, the relaxation spectrum can be obtained directly, rather than indirectly using time–temperature superposition. Such a spectrum reflects the state of the molecular dynamics of the segments, or group of segments, in the environment of other dipoles, or of nonpolar segments, in the heterogeneous or homogeneous domain [11,12].

Shears and Williams [13] were the first to observe the dielectric α relaxation, the relaxation associated with T_g,

---

[*] Corresponding author. Tel.: +1-413-545-4783; fax: +1-413-253-5295.
E-mail address: fekarasz@polysci.umass.edu (F.E. Karasz).

[1] Present address: Department of Chemical Engineering, Chemistry, and Materials Science, Polytechnic University, Six Metrotech Center, Brooklyn, NY 11201, USA.

PII: S0032-3861(01)00070-2

in mixtures of two glass-forming liquids. They found such mixtures to exhibit a broader loss peak than either of the pure components. They attributed this broadened distribution to variability in local dipole concentration. Their system was optically homogeneous, so the heterogeneities responsible for the broadening of the relaxation time spectrum were on a scale too small to scatter visible light.

Wetton et al. developed a model based on the concentration fluctuation of dipoles for the analysis of the broadened distribution of relaxation times in blends [14], whereas Ngai and Roland introduced the concept of coupled relaxation modes, to analyze their stretched exponential function quantitatively [15,16]. Fischer et al introduced a model based on concentration fluctuations of the Gaussian type that led to a broadening of the relaxation spectrum, and analyzed data obtained at various concentrations and temperatures. The results were found to be in agreement with light scattering data [17,18]. Kumar et al. also utilized a concentration fluctuation model to explain the broadening of the relaxation peak [19]. We have previously investigated the dielectric relaxation of poly *o*-chlorostyrene (PoCS), polystyrene (PS), and their blends and copolymers [20]. The relaxation spectrum of the blend was found to be generally far broader than a random copolymer of the same composition.

This study is an extension of our earlier work on the PoCS copolymers and their blends with PS. In the present work a wider frequency range from 10^{-3} to 10^{6} Hz, and a wider temperature range 370–450 K were employed permitting a more definitive analysis. Utilizing these ranges of temperature and frequency it was possible to elucidate the nature of the molecular motions near to but above T_g.

The cooperative nature of segmental relaxations characterizes the α relaxation [11,12]. This is an intermolecular process, as opposed to the intramolecular cooperative relaxation typical of the β relaxation. When polymer molecules are in a 'crowded' environment, the motion of a segment is interfered due to the presence of its neighbor. Dissipation of energetic input, typically through a rotation of the segmental bond from one stable state to another, is then possible only through the cooperation of the neighbors. Such cooperation comes in the form of a simultaneous relaxation. For two segments to move cooperatively, the probability of relaxation is squared, since each relaxation is an independent event. Thus, the cooperative relaxation time is τ^2, with τ as the relaxation time for a single segment in the absence of interference by neighbors.

At progressively lower temperatures, the volume decrease causes greater interference among neighbors. At high temperatures the cooperative relaxation involves two segments, called conformers. At lower temperatures the number involved increases to three, and then four, etc. The number of cooperating segments is defined as the size of the cooperative domain, z. This quantity occurs in the exponent of the Boltzmann probability for the relaxation rate process of Arrhenius form, so the apparent activation energy $\Delta\mu$ for the single bond rotation is multiplied by z. As z increases with decreasing temperature, the apparent activation energy increases, transforming the Arrhenius form to the Vogel–Fulcher form. The temperature at which the latter diverges is T_0, which is typically some 50 K below the empirical T_g obtained by DSC. At T_0, z is supposed to approach infinity, but before this happens, the system will deviate from equilibrium, i.e. volume, entropy and enthalpy fail to keep up with the rate of cooling, and vitrification takes place.

We have analyzed the concentration fluctuations in terms of the distribution of T_0 at a given temperature. Such a distribution is a measure of the domain size distribution, again, at that temperature. From this, we describe the concentration fluctuations in segmental terms, i.e. the local or nanoscale heterogeneity.

2. Experimental

2.1. Sample

Polystyrene (PS), molecular weight (M_w) 13,000 and polydispersity (M_w/M_n) of less than 1.06 was purchased from Pressure Chemical. Poly *o*-chlorostyrene, M_w 283,000 and M_w/M_n 1.74, and the 50 mol% copolymer (styrene/*o*-chlorostyrene) of M_w 140,000 and M_w/M_n 1.74 were purchased from Lark Enterprises. Homopolymer and copolymer films were prepared by compression molding. The blend film was prepared by solution casting using toluene as the solvent.

2.2. Dielectric measurements

Dielectric measurements were performed on a broadband dielectric spectrometer (Novocontrol GmbH). This system includes a Solatron–Schlumberger gain/phase analyzer SI1260 and high input impedance buffer amplifier (Chelsea Dielectric Interface). We were able to examine the α-process over a broad frequency (10^{-3}–10^{6} Hz) and temperature (350–450 K) range. The sample was kept at constant temperature as the frequency dependence of the complex dielectric constant was measured.

2.3. Calorimetric measurements

DSC experiments were performed on a Perkin–Elmer model DSC-7 instrument. Approximately 10 mg of sample was used, and the heating rate was 10 K/min. The DSC glass-transition values (T_g) were determined as the temperature corresponding to half of the heat capacity change. Several runs were made to ensure a uniform thermal history. This was done by first annealing the sample at 443 K for 15 min, followed by quenching to 303 K. The temperature was then raised at 10 K/min. for the measurement. A reproducible value of T_g could be obtained by this procedure.

3. Results

3.1. Thermodynamics

It is known that the polymer blend of PoCS and PS exhibits a lower critical solution temperature (LCST) [3,8,21,22]. To describe the thermodynamics of the mixing of polymers, we apply the Flory–Huggins [F–H] mean-field theory [1–3]. The Gibbs free energy of mixing, ΔG, of a mixture of two polymers according to the F–H theory can be written as

$$\frac{\Delta G}{RT} = \frac{\Phi_1}{N_1}\ln\Phi_1 + \frac{\Phi_2}{N_2}\ln\Phi_2 + \chi\Phi_1\Phi_2, \tag{1}$$

where N_1 and N_2 are the number of lattice cells occupied by polymers 1 and 2, Φ_1 and Φ_2 their volume fractions calculated on the basis of lattice occupancy, and χ is a binary interaction parameter. The binodal between two liquid phases a and b is defined by the equality of the chemical potential $\overline{\Delta G_1}$, $\overline{\Delta G_2}$ of each component in each phase

$$\overline{\Delta G_{1a}} = \overline{\Delta G_{1b}}, \qquad \text{and} \qquad \overline{\Delta G_{2a}} = \overline{\Delta G_{2b}}. \tag{2}$$

From Eq. (1) and definitions of $\partial\Delta G/\partial n_1 = \overline{\Delta G_1}$ and $\partial\Delta G/\partial n_2 = \overline{\Delta G_2}$

$$\frac{\overline{\Delta G_1}}{RT} = \frac{\ln\Phi_1}{N_1} + \left(\frac{1}{N_1} - \frac{1}{N_2}\right)\Phi_2 + \Phi_2^2\chi, \tag{3}$$

$$\frac{\overline{\Delta G_2}}{RT} = \frac{\ln\Phi_2}{N_2} + \left(\frac{1}{N_2} - \frac{1}{N_1}\right)\Phi_1 + \Phi_1^2\chi. \tag{4}$$

Thus, we have

$$\frac{\ln\Phi_{1a}}{N_1} + \left(\frac{1}{N_1} - \frac{1}{N_2}\right)\Phi_{2a} + \Phi_{2a}^2\chi = \frac{\ln\Phi_{1b}}{N_1} + \left(\frac{1}{N_1} - \frac{1}{N_2}\right)\Phi_{2b} + \Phi_{2b}^2\chi, \tag{5}$$

$$\frac{\ln\Phi_{2a}}{N_2} + \left(\frac{1}{N_2} - \frac{1}{N_1}\right)\Phi_{1a} + \Phi_{1a}^2\chi = \frac{\ln\Phi_{2b}}{N_2} + \left(\frac{1}{N_2} - \frac{1}{N_1}\right)\Phi_{1b} + \Phi_{1b}^2\chi. \tag{6}$$

It is necessary to use approximation methods to calculate χ from Eqs. (5) and (6) since the equations diverge at $\Phi_{2a}^2 = \Phi_{2b}^2$, and $\Phi_{1a}^2 = \Phi_{1b}^2$. In order to do this a suitable value of Φ_{2b} is selected, and a trial value for Φ_{2a} is assumed. Then, $\Phi_{1a} = 1 - \Phi_{2a}$; $\Phi_{1b} = 1 - \Phi_{2b}$, and all quantities in Eqs. (5) and (6) are known except χ. We calculated χ from Eq. (5) as χ_1, and from Eq. (6) as χ_2, and varied Φ_{2a}. χ was determined at the minimum value of $|\chi_1 - \chi_2|$. A suitable starting value of Φ_{2b} can be derived from the location of the critical concentration at $\partial^2\Delta G/\partial\Phi_1^2 = \partial^3\Delta G/\partial\Phi_1^3 = 0$, which is expressed by

$$\Phi_{2c} = 1/\{1 + (N_2/N_1)^{1/2}\}. \tag{7}$$

The value of χ at the critical condition is [1–3]

$$\chi_c = \frac{1}{2}(N_1^{-1/2} + N_2^{-1/2})^2. \tag{8}$$

The calculated value of χ_c for our sample is 0.007.

The spinodal is obtained from the condition $\partial^2\Delta G/\partial\Phi^2 = 0$ as

$$\chi = \frac{1}{2}\left(\frac{1}{N_1\Phi_1} + \frac{1}{N_2\Phi_2}\right). \tag{9}$$

Unlike the binodal case, Eq. (9) can be solved explicitly for χ in a straightforward manner. In Fig. 1(a), the binodal and spinodal boundaries for blends of PS (13,000) and PoCS (283,000) are shown calculated by the above procedures.

The temperature dependence of χ can be described as follows [3,4]:

$$\chi(T) = A\frac{B}{T} + CT + D\ln T, \tag{10}$$

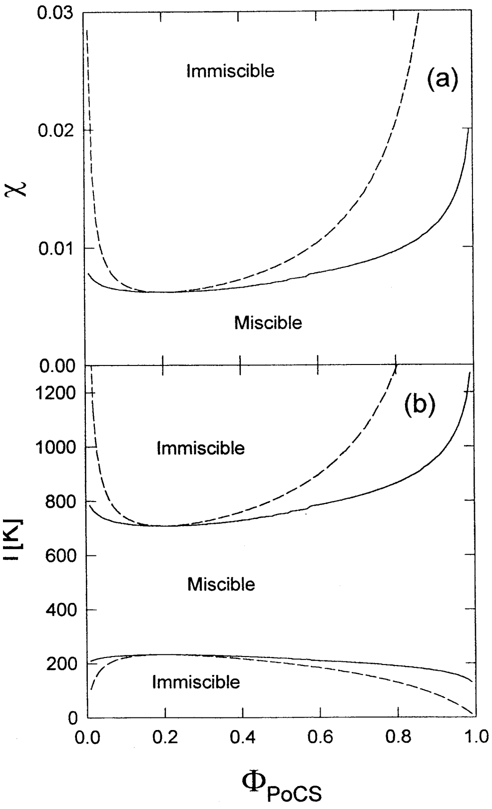

Fig. 1. Phase diagram of (a) χ vs Φ, and (b) T (K) vs Φ for polymer blends of polystyrene (MW 13,000) and poly o-chlorostyrene (MW 283,000). The solid line is the binodal boundary calculated from Eqs. (5) and (6), and the dotted line is the spinodal boundary calculated from Eq. (9).

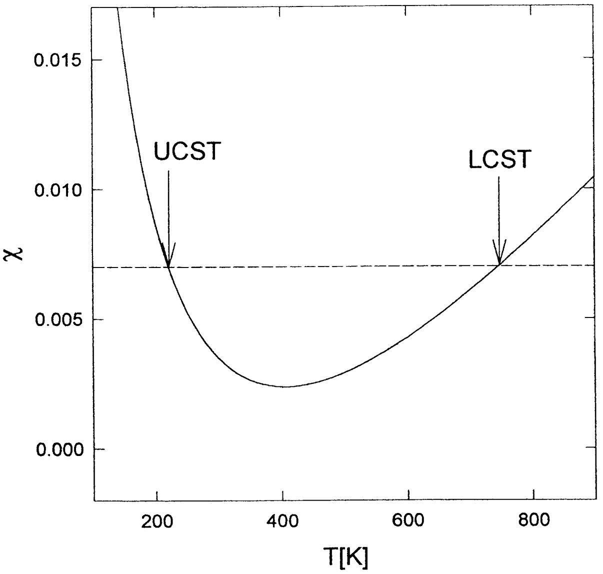

Fig. 2. Temperature dependence of χ for PoCS/PS polymer blends as given by Ref. [8]. The UCST and LCST in a blend with $\chi_c = 0.007$ are shown schematically.

where A, B, C, and D are constants, which can be obtained for blends of PS and PoCS experimentally and, whose values are $A = -2.17 \times 10^{-2}$, $B = 4.89$, $C = 2.97 \times 10^{-5}$; D is negligible [8]. The temperature dependence of χ, indicating the presence of both LCST and UCST for $\chi_c = 0.007$ is shown in Fig. 2. The phase diagram of temperature versus Φ_{PoCS} was calculated using Eq. (10) as shown in Fig. 1(b). Based on this and earlier experimental results on a comparable blend [23,24], the PS (13,000)/PoCS (283,000) blend should be miscible below 443 K.

DSC data on the 50% blend of PoCS and PS showed a single T_g after annealing at 443 K. The samples did not experience a temperature substantially above the LCST before quenching. The UCST was not observed, since the critical temperature is below T_g. The measured glass transition temperatures of PS, PoCS, 50 mol% PoCS/PS blend and 50 mol% P(oCS/S) copolymers are listed in Table 1.

Strictly speaking, the analysis embodied in Eqs. (1)–(9) applies only to a binary system. Since a distribution of molecular weights exists, this is obviously an approximation. However, it can be shown that the analysis used here affects only the binodal boundary and the qualitative conclusions remain unaltered.

Table 1
Vogel–Fulcher parameters for PoCS, PS, PoCS/PS blend, P(oCS/S) random copolymer

Sample	$\log f^*$ (Hz)	$\Delta\mu^*$ (kJ/mol)	T_0 (K)	T_g (K)	
				($\tau^* = 1$ s)	(DSC)
PoCS	9.1	11.3	342	392	397
PS	10.5	12.7	327	379	381
PoCS/PS	9.7	12.9	335	391	391
P(oCS/S)	9.4	11.2	331	382	383

3.2. Assignment of the relaxation process

The broadband dielectric measurements were made on samples of PS, PoCS, a 50 mol% PoCS/PS blend, and a 50 mol% P(oCS/S) random copolymer, at temperatures between 370 and 450 K. A single relaxation process was observed in each case. The frequency dependencies of ϵ' and ϵ'' for the blend are shown in Fig. 3 and those for the copolymer are shown in Fig. 4. Both blend and copolymer show increases in the maximum values of ϵ'' with increasing temperature, and both exhibits narrowing in the frequency range of ϵ'' with increasing temperature. However the frequency dependencies of ϵ'' for the blend remain low and broad until much higher temperatures than in the case for the copolymer. It is the object of this study to elucidate these differences quantitatively.

The frequency of the loss maximum, $f_{\max}$, is plotted against the reciprocal of the absolute temperature $1/T$ in

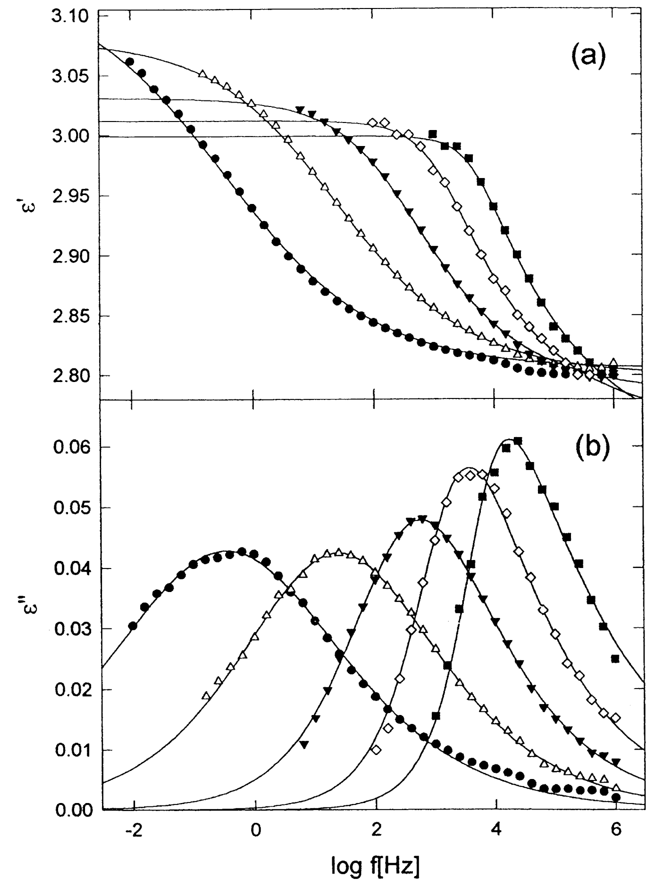

Fig. 3. Frequency dependence of (a) ϵ' and (b) ϵ'' for 50 mol% PoCS/PS blend at various temperatures: (●) 393 K; (△) 403 K; (▼) 413 K; (◇) 423 K; (■) 433 K. Solid lines are fits to the Havriliak–Negami function of Eq. (12).

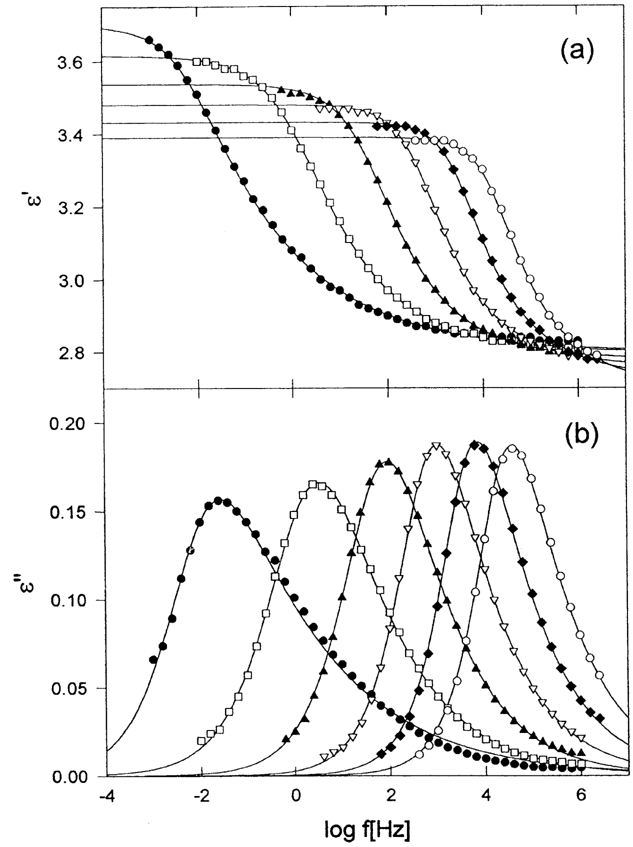

Fig. 4. Frequency dependence of (a) ϵ' and (b) ϵ'' for 50 mol% P(oCS/S) copolymer at various temperatures: (●) 378 K; (□) 388 K; (▲) 398 K; (▽) 408 K;(◆) 418 K; (○) 428 K. Solid lines are fits to the Havriliak–Negami function of Eq. (12).

Fig. 5. The experimental temperature dependence of $f_{\max}$ was then fitted to the Vogel–Fulcher equation [25,26]

$$\log f_{\max} = \log f^* - \frac{\Delta\mu^*}{R/\log e}\left[\frac{1}{T-T_0} - \frac{1}{T^*-T_0}\right], \qquad (11)$$

where f^* is the frequency of the loss maximum at a reference temperature T^*. At the divergence temperature T_0 the cooperative entropy approaches zero, though the conformational entropy is far from zero [12]. $\Delta\mu^*$ is the Vogel–Fulcher energy, which is interpreted as the activation energy barrier to the rotation of a single conformer. The characteristic relaxation time τ is equal to $1/2\pi f_{\max}$. The Vogel–Fulcher parameters were evaluated from the data, and are shown in Table 1.

The relaxation process observed is the α-process corresponding to the cooperative relaxation of the conformers related to the micro-Brownian motion of the main chain. The observed values of τ in PS and PoCS homopolymers are in agreement with the reported values [20,27], and the temperature dependence of $f_{\max}$ follows the Vogel–Fulcher equation. By defining the T_g as the temperature at which the dielectric τ is 1 s, agreement is obtained with the DSC T_g as shown in Table 1. The values of T_0 are about 50 K lower than T_g as expected. The Vogel–Fulcher activation energies, $\Delta\mu$, of the blend, the copolymer and the homopolymer of PS are in good agreement with the reported values of about 12–15 kJ/mol.

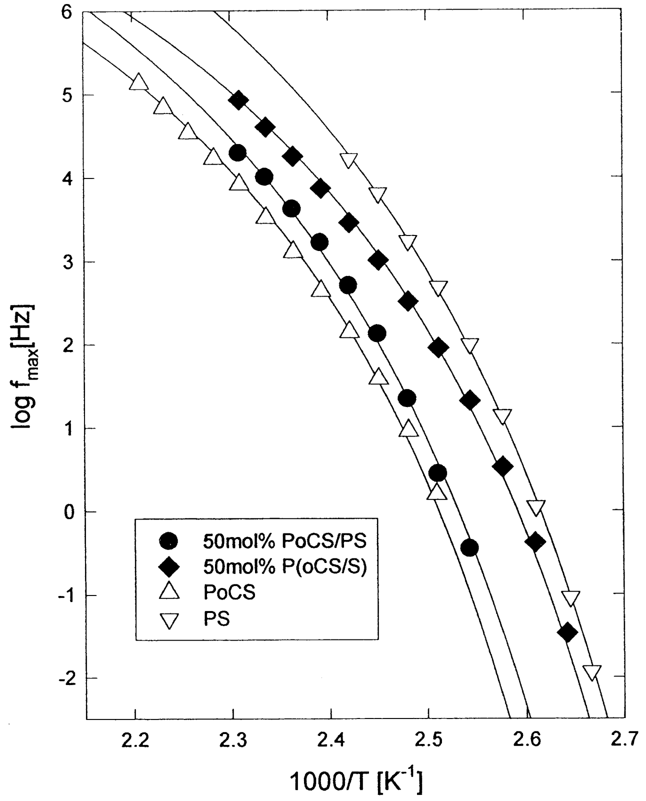

Fig. 5. Plots of log frequency of the dielectric loss maximum, $\log f_{\max}$ (Hz), against the reciprocal of the absolute temperature: (△) PoCS; (▽) PS; (●) 50 mol% PoCS/PS blend; (◆) 50 mol% P(oCS/S) copolymer. Solid lines are calculated from Eq. (11).

3.3. Comparison of dielectric relaxation curves of polymer blends and copolymers

The frequency dependence of the complex permittivity ϵ^* is frequently described by the empirical Havriliak–Negami representation [28]

$$\epsilon^*(\omega)\epsilon'(\omega) - j\epsilon''(\omega) = \frac{\Delta\epsilon}{\{1+(j\omega\tau_{HN})^{\beta}\}^{\alpha}} + \frac{\sigma_{dc}}{j\omega\epsilon_0} + \epsilon_\infty, \qquad (12)$$

where $\epsilon'(\omega)$ is the real part of the dispersion, $\epsilon''(\omega)$ the imaginary part, ϵ_∞ the dielectric constant at $\omega \to \infty$, $\Delta\epsilon$ the relaxation strength, τ_{HN} the characteristic relaxation time of the Havriliak–Negami equation, ϵ_0 the dielectric constant of vacuum, j the imaginary unit and σ_{dc} is the dc conductivity. The Havriliak–Negami parameters were determined by a fitting procedure using WinFit (Novocontrol GmbH) software. After σ_{dc} was subtracted from the total spectrum, the results are the solid lines shown in Figs. 3 and 4. The variables α and β of Eq. (12) are empirical parameters

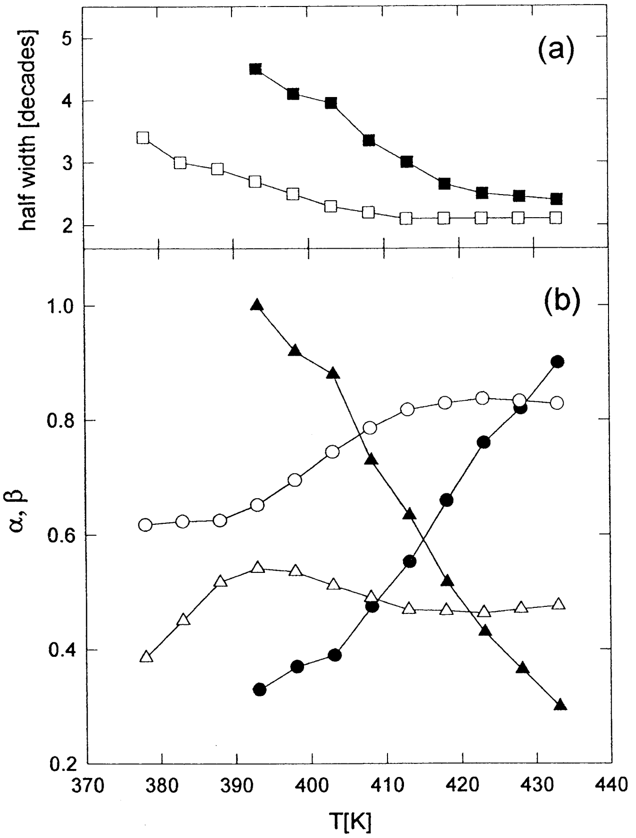

Fig. 6. Temperature dependencies of (a) half width of $\epsilon''(\omega)$, and (b) α and β in Eq. (12): (■) half width of 50 mol% PoCS/PS blend; (□) half width of 50 mol% P(oCS/S) copolymer; (●) α of PoCS/PS; (▲) β of PoCS/PS; (○) α of P(oCS/S); (△) β of P(oCS/S).

that are related to the distribution of relaxation times. If the dipoles are able to orient independently, α and β should be unity, and the process is of the Debye, single relaxation time, type. In a system where correlation between dipoles exists, there is a distribution of relaxation times and α and β are less than unity. One illuminating aspect of the α and β parameters is that ϵ'' on the high frequency side of the peak is proportional to $\omega^{\alpha\beta}$, which is related to the distribution of domain sizes smaller than z, the maximum size that is a function of the temperature [12].

Temperature dependencies of the half widths, α and β for the dispersions are shown in Fig. 6. The dispersion of the polymer blend is much broader than that of the corresponding copolymer, in agreement with previous results [20]. The temperature dependencies of α and β for the blend PoCS/PS reflect the large temperature dependencies of the shape of the relaxation spectrum.

For comparison of the relaxation curves, the logarithm of the dielectric loss spectra as a function of the logarithm of frequency for PoCS/PS at 403 K and P(oCS/S) at 388 and 393 K are shown in Fig. 7. The slope on the high frequency side of the peak is an indication of the distribution of the domain sizes [12], whereas the lower frequency side is affected by the distribution of T_0 s on the domain scale.

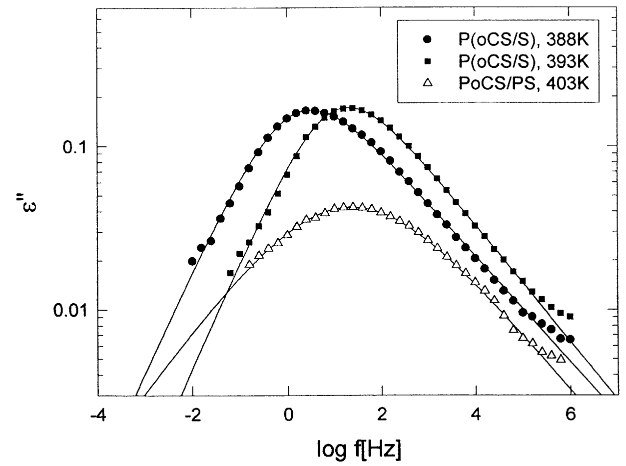

Fig. 7. Logarithm of the frequency dependences of ϵ'' for 50 mol% PoCS/PS blend at (△) 403 K and 50 mol% P(oCS/S) copolymer at (●) 388 K and (■) 393 K. Solid lines are fits to Havriliak–Negami function of Eq. (12).

This will be discussed in more detail below. A qualitative observation can be made regarding the comparison of the copolymer and the blend. First, the absorption strength is low for the blend, and this indicates the effective dipole moment and/or the population of the effective dipoles is smaller than in the copolymer. Analysis of the g-factor below gives more information about the effective dipole moment. Second, a broader distribution of the relaxation times is seen in the blend compared to the copolymer, as noted by other workers. This will be analyzed by adopting a cooperativity model to estimate the difference in the distribution of domain sizes between the copolymer and the blend. Additional points are made by viewing the same data in the normalized form relative to the peak height, as shown in Fig. 8. Although relaxation curves become broader even in the copolymer as the temperature is decreased, such

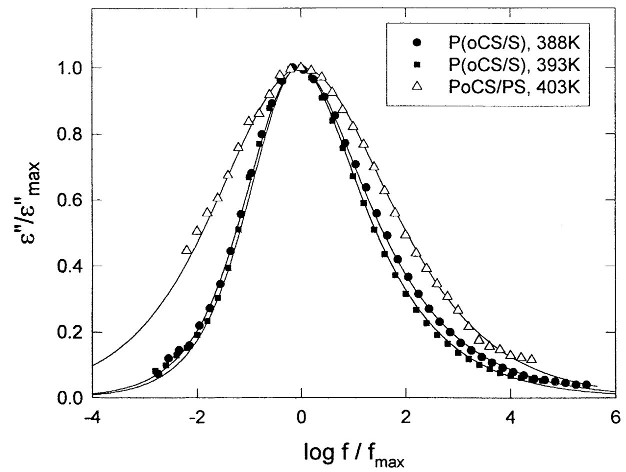

Fig. 8. Normalized frequency dependencies of ϵ'' for 50 mol% PoCS/PS blend at (△) 403 K and 50 mol% P(oCS/S) copolymer at (●) 388 K and (■) 393 K, where $f_{\max}$ is the frequency at the dielectric loss maximum $\epsilon''_{\max}$. Solid lines are fits to the Havriliak–Negami function of Eq. (12).

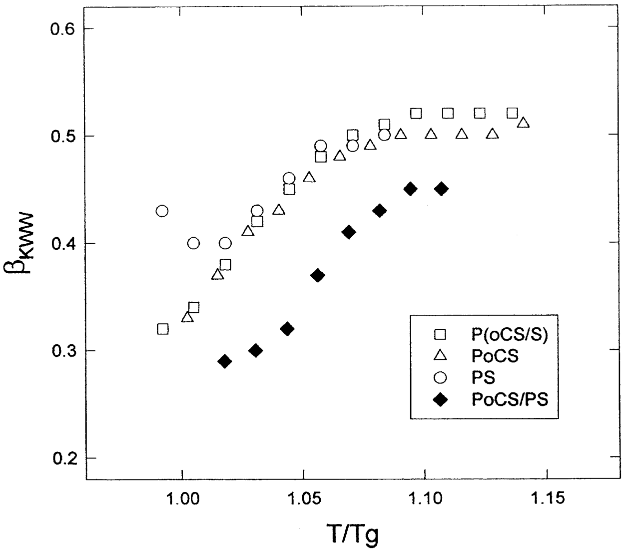

Fig. 9. Plots of β_{KWW} against normalized temperature: (◆) 50 mol% PoCS/PS blend; (□) 50 mol% P(oCS/S) copolymer; (△) PoCS homopolymer; (○) PS homopolymer.

broadening is small compared to the broad peak of the blend.

To consider the concentration dependence of domain size in the blends, we have analyzed the shape of the relaxation peak with fits to the Kolrausch–Williams–Watts (KWW) function [9]

$$\epsilon^*(\omega) - \epsilon_\infty = \Delta\epsilon \int_0^\infty \exp(\mathrm{j}\omega t)\left[\frac{-\mathrm{d}\varphi(t)}{\mathrm{d}t}\right]\mathrm{d}t \tag{13}$$

and

$$\varphi(t) = \exp[-(t/\tau_{\mathrm{KWW}})^{\beta_{\mathrm{KWW}}}], \qquad 0 < \beta_{\mathrm{KWW}} < 1,$$

where τ_{KWW} is the characteristic relaxation time of the KWW function, and β_{KWW} is the KWW parameter to describe the peak shape. The plots of β_{KWW} for the copolymer of 50 mol% P(oCS/S), and homopolymers of PS and PoCS against temperature, normalized to T_g, are shown in Fig. 9. The differences among P(oCS/S), PS and PoCS are relatively small above $T_g + 10$ K. This indicates that the peak shape of the copolymer at any concentration can be expected to be close to that of the homopolymer. For reference, β_{KWW} for blends of 50 mol% PoCS/PS is also plotted in Fig. 9, although the fit to the equation is not good in the temperature region below 408 K.

4. Discussion

4.1. Deconvolution of the broadened loss peak

We begin this section with an analysis of the peak shape. If we assume that the broadened α relaxation can be considered as a result of superposition of relaxation mechanisms, the loss factor $\epsilon''(\omega)$ can be obtained from the distribution function $P(\tau)$ as follows [9,27]:

$$\epsilon''(\omega)/\epsilon''_{\mathrm{max}} = \int_{-\infty}^{\infty} P(\tau)\frac{\omega\tau}{1+\omega^2\tau^2}\,\mathrm{d}\log\tau. \tag{14}$$

If the distribution is mainly due to dipole concentration fluctuations, then the function $P(\tau)$ should be the normal distribution function around τ_{max}, i.e.

$$P(\tau) = \frac{1}{\sqrt{2\pi}\sigma}\exp\left\{-\frac{(\log \tau/\tau_{\mathrm{max}})^2}{2\sigma^2}\right\}, \tag{15}$$

where σ is the standard deviation of the normal distribution above. In our study, we are concerned with concentration fluctuations in the blends. If we assume $P(\tau)$ to be exclusively due to local variations in the concentrations of PS and PoCS, then we must treat the dipole concentration fluctuation as a separate factor. To do this, we take the frequency dependence of ϵ'' for the pure copolymer of 50 mol% composition to represent the distribution of dipole concentration fluctuations in a homogeneous segmental mixture of PC and PoCS. Thus substitution of the kernel $\{\omega\tau/(1+\omega^2\tau^2)\}$ in Eq. (14) by $\{K\epsilon_{\mathrm{A}}''(\omega\tau)\}$ from the experimental results for the 50 mol% copolymer leads to

$$\epsilon''(\omega)/\epsilon''_{\mathrm{max}} = K\int_{-\infty}^{\infty} P(\tau)\epsilon''_{\mathrm{A}}(\omega\tau)\,\mathrm{d}\log\tau, \tag{16}$$

where $\epsilon''_{\mathrm{A}}(\omega)$ is the experimentally obtained dielectric loss factor of copolymer P(oCS/S) at the same temperature as the polymer blends being analyzed.

In practice, the integral of Eq. (16) can be replaced by a sum of terms

$$\epsilon''(\log\omega) = K\Delta\log\tau \sum_{n=-20}^{20} P(n\Delta\log\tau)\epsilon''_{\mathrm{A}}(\log\omega - n\Delta\log\tau), \tag{17}$$

where n is a whole number, and $\Delta\log\tau$ is 0.2, the same as the interval of the experimental data. The lower and upper limits of n were chosen to yield a sufficient range of $\omega\tau$ to cover the whole relaxation process in the blend. There are 41 integer values of n between −20 and 20. We considered 41 different concentrations of blends, each having a different f_{max}. Each ϵ'' was shifted along the $\log\tau$ axis by $n\Delta\log\tau$ from the center, $\log f_{\mathrm{max}}$ for the whole blend. Each of the ϵ''_{A} $(\log\omega - n\Delta\log\tau)$ terms was weighted according to the $P(\log\tau)$ function to account for the concentration distribution in the blend. This procedure is illustrated in Figs. 10 (a) and (b).

From the above analysis, the following statements may be made:

1. The broader spectrum of relaxation times for the blend than for the copolymer is due to the concentration fluctuation of the homopolymers in the blend being greater than those of the copolymer i.e. mixing in the blend is not as uniform as in the copolymer.
2. While the spectrum of the pure copolymer becomes

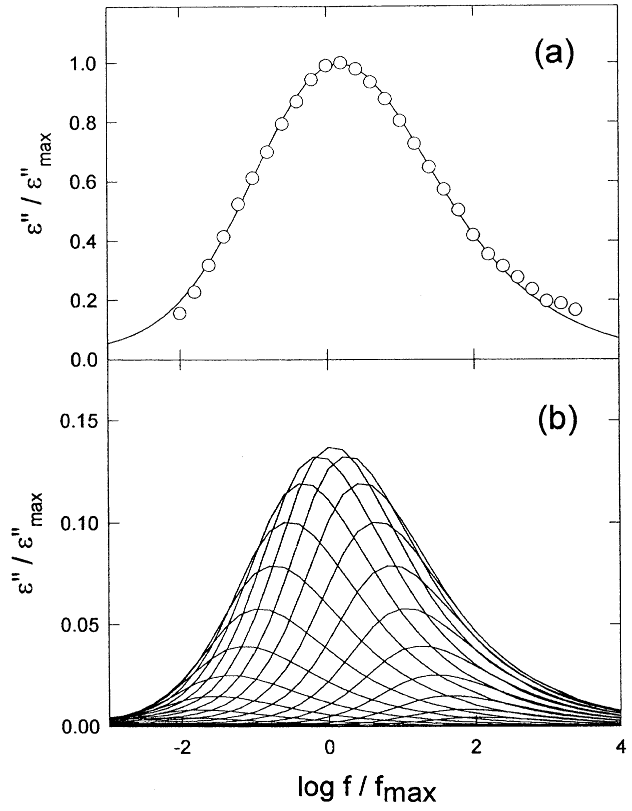

Fig. 10. (a) Normalized frequency dependence of ϵ'' for 50 mol% PoCS/PS blend at 413 K fitted with Eq. (17). (b) Deconvoluted spectrum of the numbers between $-10 < n < 10$ in Eq. (17). The shape of each spectrum is the same as that of the copolymer at 403 K. Summation of these spectra produces the solid line of (a).

broader at lower temperatures, the concentration fluctuations in the blend also become greater, as shown by the temperature dependence of σ.

3. As a corollary to (2), the random copolymers of the same composition could exhibit different degrees of broadening, depending on the sequence propagation constant, i.e. the size of the heterogeneities.

The frequency dependence of $\epsilon''(\omega)$ is normalized by log ω/log $\omega_{\max}$ before the calculation of Eq. (17). The standard deviation, σ of $P(\tau)$, which is the only variable in the equation, was determined by the least-square mean procedure to find the best fit. The $\epsilon''(\omega)/\epsilon''_{\max}$ obtained at each temperature can be well represented by Eq. (17). An example is given for the blend at 413 K, in Fig. 10. The width factor, or the standard deviation, σ, changes with temperature. The curve becomes broader at lower temperatures. The temperature dependence of the width parameter σ is shown in Fig. 11. The plots of $P(\log \tau)$ as functions of log τ are shown in Fig. 12.

The origin of the broadening has been assumed to arise from the effective distribution of local concentration fluctuations by many authors [13–20,29]. However, their procedures for the quantitative estimation of the scale of the concentration fluctuations differ. The convolution integral of Eq. (14) was introduced by Shears and Williams [13] for the first time, and developed by Wetton et al. [14]. The former utilized the Fuoss–Kirkwood equation for $\epsilon''_A(\omega)$ and a rectangular function for $P(\tau)$. The rectangular function was replaced by the normal distribution function by Wetton et al. Fischer et al. used the Havriliak–Negami equation with α and β obtained from the homopolymer [17,18]. Ngai et al. assumed that concentration fluctuations produce a Gaussian distribution of the coupling parameters, reflecting the cooperative dynamics of various local environments arising from the concentration fluctuation [15,16].

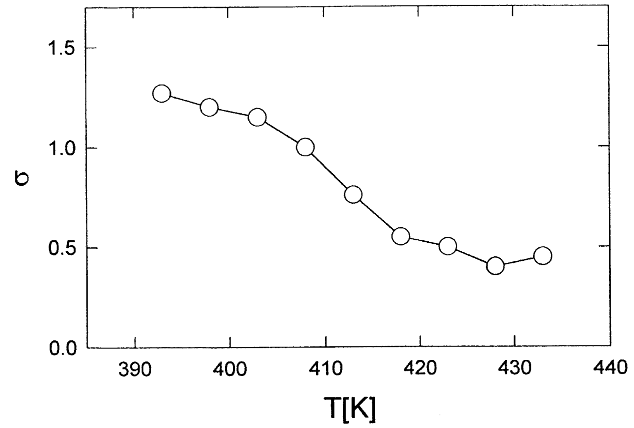

Fig. 11. Temperature dependence of width parameter σ in Eq. (15).

4.2. Adopting the model of intermolecular cooperativity

We now wish to consider the nature of concentration fluctuations affecting the relaxation behavior of blends, adopting the model of intermolecular cooperativity [11,12]. In the presence of mechanical or electrical stress, a polymer molecule changes its unperturbed conformation to a less random conformation. The overall conformational change is the sum of rotations of bond angles in the main chain. To pass from one stable state to another, the bond angle must pass through a transient high-energy state. The

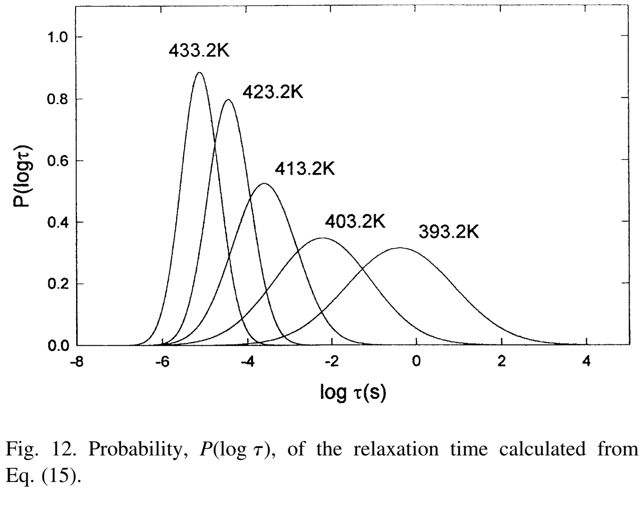

Fig. 12. Probability, $P(\log \tau)$, of the relaxation time calculated from Eq. (15).

probability for this high-energy state is the rate determining factor, and the chemical potential $\Delta\mu$ elevated from the initial state is the activation energy for the relaxation. The relaxation time τ is inversely proportional to the probability of reaching that energy barrier. If the relaxation time at some reference temperature T^* is defined as τ^*, then the relaxation time τ at another temperature T is given by

$$\tau = \tau^* \exp\left(\frac{\Delta\mu}{RT} - \frac{\Delta\mu}{RT^*}\right), \tag{18}$$

where R is the universal gas constant. We call the rotational unit a conformer, the smallest unit necessary for a conformational change.

In the condensed state, there is another factor that affects the relaxation time, and that is the interference from the neighbors that becomes increasingly important as the temperature is decreased. In the densely packed state it is assumed the rotation of a bond into a new angle is often prevented by collision with a neighbor. To succeed, the rotation of the neighboring conformers must occur simultaneously. The probability for z conformers to relax simultaneously is the zth power of the individual probabilities. The cooperative relaxation time is τ^z. Taking a high enough reference temperature T^* at which z is 1, the cooperative relaxation time is given by the formula [30]

$$\tau = \tau^* \exp\left(\frac{\Delta\mu}{RT} z - \frac{\Delta\mu}{RT^*}\right). \tag{19}$$

T^* is the temperature at which the relaxation is as fast as the frequency of the stress cycle, i.e. $T^* \sim \Delta\mu/R$. As $\Delta\mu$ is about 3 kcal/mol, T^* should be about 750 K. We found T^* of 773 K (500°C) and τ^* of 3×10^{-12} s to be good values for a large number of polymers [11,12].

The temperature dependence of z is calculated from the ratio of an extensive quantity such as the entropy or the free volume with and without cooperativity.

The free volume can be considered to be the van der Waals excess volume, V_f, that is the difference between the liquidus and the solid volume. The latter is the crystalline volume, if the substance can be crystallized. If not, it may be estimated. The 'occupied' volume of the glassy 'state' is substantially greater, as it will be shown to be related to the cooperative relaxation. The free volume fraction $f = V_f/V$ is often given by the formula:

$$f = \Delta\alpha T, \tag{20}$$

where $\Delta\alpha$ is the difference in the thermal expansion coefficients of the liquidus and the crystalline states.

The domain of cooperativity, z, grows larger as the temperature is decreased until it becomes large enough and the relaxation time is so great that the structural change cannot keep up with the decreasing temperature. This point represents the glass transition, and the temperature at which a transition occurs to a glassy non-equilibrium state is called the fictive temperature. The fictive temperature is lower if the cooling is slower which also results in a denser structure for the annealed glassy state. T_g, as measured by DSC will be higher for a more highly aged glass, because of the overshoot due to the greater relaxation time of the aged glassy state. The fictive temperature is at the border of equilibrium and non-equilibrium states, whereas T_g measured by DSC is not a thermodynamic quantity.

With decreasing cooling rates, the fictive temperature decreases, until finally, at the zero rate of cooling, z approaches infinity. The phenomenological temperature T_0 is defined as the fictive temperature for the infinitely slowly cooled glass. Concurrently, the fractional free volume has decreased, but not to zero at T_0. While there still remains a certain amount of free volume, the interference among the neighbors has spread to the entire system, and cooperative relaxation has become impossible. The fractional free volume at T_0 is defined as f_0.

At T below T^* but above T_0, the cooperative fractional free volume f_{coop} is given by

$$f_{coop} = f - f_0 = \Delta\alpha(T - T_0). \tag{21}$$

The domain size z is proportional to the ratio f/f_{coop}, because the mol fraction of domains is equal to $1/z$. Hence $z\mu f/(f - f_0)$. However, z must be 1 at T^* by the definition of the latter. Hence the temperature dependence of z is given by the equation

$$z = \frac{T}{T - T_0}\,\frac{T^* - T_0}{T^*}. \tag{22}$$

Substitution of Eq. (22) into Eq. (19) gives the familiar Vogel–Fulcher equation

$$\tau = \tau^* \exp\left(\frac{\Delta\mu^*}{R(T - T_0)} - \frac{\Delta\mu^*}{R(T^* - T_0)}\right), \tag{23}$$

where $\Delta\mu^* = \Delta\mu(T^* - T_0)/T^*$.

The above equation can also be derived by considering the entropy instead of the free volume. In that case, the domain size is proportional to the ratio of the conformational entropy S, and the cooperativity entropy S_{coop}. This will result in the Adam–Gibbs formulation [30] for the cooperative relaxation time, from which the Vogel–Fulcher form of Eq. (11) can be again obtained.

By considering f_0 as the 'occupied' volume fraction, one can derive Doolittle's [31] free volume equation, and further, the Williams–Landel–Ferry (WLF) equation from the Vogel–Fulcher equation, Eq. (23). Ferry et al. [32] found the universal WLF equation with the same parameters applicable to many polymers, when T_g is chosen as the reference temperature. It can be shown that this implies that $T_g - T_0$ amounts to 50 K.

We have thus shown that T_0 is determined by the extra amount of free volume and entropy required for cooperativity. This does not, however, explain why T_0 and T_g vary, sometimes widely, from material to material.

One point that has not been included in the above calculation is the fact that entropy depends on the molar volume.

The entropy decreases with increasing density, even if the conformation is kept unchanged. The probability of the spatial arrangements is dependent on the free volume, similar to the way the entropy of the ideal gas depends on the volume. For the ideal gas, this entropy is equal to $k\ln V$. For the free volume, this would be $k\ln V_f$. The absolute molecular volume has now entered in the calculation of T_0. When the temperature is changed from T^* to T_0, this volume-related entropy decreases in proportion to the logarithm of the molecular volume, which varies with the size of the conformer. To set T_0 as the critical temperature at which this entropy reaches the same critical value for all polymers of different conformer size, the following proportionality can be established between polymer A and polymer B

$$(T^* - T_{0,A}) \ln M_A = (T^* - T_{0,B}) \ln M_B = c_3, \tag{24}$$

where M_A, and M_B are the molecular weights of conformers A and B, and $T_{0,A}$ and $T_{0,B}$ are the corresponding T_0; c_3 should be a constant for all polymers. This equation states, quantitatively, that a large conformer has a higher T_g. This equation has been supported empirically for more than 50 polymers, with the values $c_3 = 1750$, and $T^* = 773$ K [11].

We can now apply Eq. (24) to PS and PoCS. The average conformer sizes are $104/2 = 52$ and $139/2 = 68$, respectively, and thus $T^* - T_0$ of 443 and 415 K are obtained. With $T^* = 773$ K, T_0 of 330 and 358 K are obtained. If $(T_g - T_0)$ is assumed to be 46 instead of 50 K,[2] the corresponding T_g of 376 and 404 K are obtained, in agreement with the data obtained by thermal analysis [20].

For the blend of PoCS and PS homopolymers, those domains that are rich in PoCS are larger than those rich in PS, not only in the average size of conformers but also in the number per domain, z. The frequency dispersion in ϵ'' is due to this difference among those domains with different sizes. It increases at lower temperatures, because the z of the PoCS rich domains grows faster than the z of the PS domains. For example, z for PS and PoCS are 2.41 and 3.10 at 433 K, 2.85 and 4.03 at 413 K, and 3.57 and 6.03 at 393 K, respectively. The corresponding broadening toward the lower temperatures is seen for the probability function $P(\log \tau)$ as shown in Fig. 12. The breadth of $P(\log \tau)$ rapidly increases at lower temperatures.

In the copolymer of the same composition as the blend this broadening is not observed, at least in this temperature range. It means that the domain of cooperativity remains more uniform. It is an indication that the sequence propagation is short with respect to aggregates of concentration fluctuations. If the sequence length of each co-monomer unit is made longer, eventually it will approach a block copolymer and $\epsilon''(\omega)$ should exhibit a broadening tendency similar to that of the blend.

Although the following alternative explanation will be less likely for this blend in the temperature range considered, there is another possible cause for broadening of the loss peak, and it is related to the distribution of the domain size z being fixed in the non-equilibrium glassy state. There is always a fluctuation in the size of the domains, even in a homopolymer. When the temperature is below T_g, the size distribution remains frozen and a wide difference in the activation energy levels, $\Delta\mu z_i$ for $i = 1, 2, 3$, etc. will broaden the relaxation process at lower temperatures. A domain of cooperativity that consists totally of PoCS conformers may begin to show a broader peak below 413 K on its own, while a domains rich in PS will remain as typical of the equilibrium state. Thus the difference between the characteristic relaxation times of the PoCS rich domains and PS-rich domains will widen, purely as a consequence of the higher glass transition of the pure PoCS component. We believe that this is unlikely to be the case here, because the copolymer did not show a broadening tendency in the same temperature range.

4.3. Analysis of effective dipole moment

The intensity of the loss peak of the polymer blend is apparently smaller than that of the copolymer as shown in Fig. 8, although the concentration of oCS units in the blend is the same as that in copolymer. To consider this difference, we estimated the structural factor (g-factor) from the relaxation strength. The effective dipole moment μ_e per repeat unit is calculated from the Onsager equation [33]

$$\mu_e^2 = \frac{9kT}{4\pi N} \frac{\Delta\epsilon(2\Delta\epsilon + 3\epsilon_\infty)}{(\Delta\epsilon + \epsilon_\infty)(\epsilon_\infty + 2)^2}, \tag{25}$$

where N is the number of dipoles per unit volume, and k is the Boltzmann constant. The reported values [34] of 1.25 and 1.05 g/cm^3 have been used for the densities of PoCS and PS. The densities of the PoCS/PS blend and P(oCS/S) copolymer were obtained by assuming the validity of the following relationship:

$$1/\rho = (W_1/\rho_1) + (W_2/\rho_2), \tag{26}$$

where the W_1 and W_2 are the weight fractions, and ρ_1 and ρ_2 are the densities of the homopolymers. Then N is obtained from

$$N = N_A \rho/(X_1 M_1 + X_2 M_2), \tag{27}$$

where N_A is Avogadro's number, X_1 and X_2 the mole fractions, and M_1 and M_2 are the molecular weights of the repeat unit. The Kirkwood–Frohlich dipole correlation factor, g, was determined from

$$g = \mu_e^2/\mu_0^2, \tag{28}$$

where

$$\mu_0^2 = X_1\mu_1^2 + X_2\mu_2^2$$

---

[2] The value of T_g depends on the technique and the method of analysis. $(T_g - T_0)$ of 46 K was chosen here instead of 50 K, to make a comparison between PS and PoCS in relation to a set of data in Ref. [20].

Table 2
Effective dipole moment and *g*-factor for PoCS, PS, PoCS/PS blend, P(oCS/S) random copolymer

Sample	μ_V^2 (D)	μ_E^2 (D)	*g*
PoCS	2.43	0.68	0.28 ± 0.02
PS	0.13	0.03	0.23 ± 0.02
PoCS/PS	1.28	0.25	0.19 ± 0.02
P(oCS/S)	1.28	0.65	0.52 ± 0.02

and μ_0 is the dipole moment of the repeat unit, μ_1 and μ_2 are the gas-phase dipole moments of toluene ($0.36D$) and *o*-chlorotoluene ($1.56D$), respectively. The obtained effective dipole moment and *g*-factors of PS, PoCS, 50 mol% P(oCS/S) and 50 mol% PoCS/PS are listed in Table 2. The temperature dependence of the *g*-factor is small in all of the samples. The standard deviations in the whole temperature region are also shown as error limits in Table 2.

The *g*-factor is given by $1 + m\langle\cos\gamma\rangle$, where m is the average number of nearest neighbor dipole moments, and $\langle\cos\gamma\rangle$ is the average of the cosine of the angle between neighboring dipoles. If the dipole is isolated, $g = 1$. The *g*-factor of the 50 mol% copolymer is closer to unity than those of the homopolymers of PS and PoCS. This is explained by the fact that the polar *o*-chlorostyrene units are diluted by the relatively nonpolar styrene units, since the *o*-chlorostyrene unit is dispersed homogeneously. However, the *g*-factor of the polymer blends is nearly the same as those of PS and PoCS. This means that the local conformational states of the PoCS chain are not perturbed by blending with PS, and the mixing of PoCS with PS does not occur on a segmental scale.

5. Conclusions

In this paper we have attempted to describe the effects of concentration fluctuations on the cooperativity in segmental motions from dielectric relaxation measurements carried out on the polymer blend 50 mol% PoCS/PS, the copolymer 50 mol% P(oCS/S), and the homopolymers PS and PoCS. The dielectric relaxation spectrum of the polymer blend has been compared with that of the copolymer. The observed relaxation process was assigned to the α process due to segmental motion in each case, since the temperature dependence of the frequencies of the observed loss maxima was of the Vogel–Fulcher type. The shape of the relaxation dispersion of the polymer blend was broader than that of the copolymer due to mixing heterogeneity in the former at the segmental level. The relaxation dispersion for the blend was deconvoluted to extract various relaxations arising from different local concentrations. The shape of the curve at each concentration was obtained from the copolymer spectrum at the same temperature, which was taken to represent the relaxation of a homogeneous system. We did not need to consider concentration effects since the peak shape of the copolymer was nearly the same as those of homopolymers of PS and PoCS. The probability, $P(\log\tau)$, for the peak positions of the deconvoluted process, which can be regarded as the distribution of relaxation times, was represented by a Gaussian distribution. The distribution, $P(T_0)$ of the Vogel–Fulcher temperatures, T_0, was estimated from $P(\log\tau)$ by the Vogel–Fulcher equation. For reference, $P(T_0)$ at 418 K is shown in Fig. 13. In this treatment, $P(T_0)$ can be regarded as a criterion for the existence of heterogeneity at the segmental level. For example, if $P(T_0)$ transforms to the distribution $P(z)$ of the cooperative domain size, adopting the model of intermolecular cooperativity, the heterogeneity of the cooperative motion can be observed at each temperature. The *g*-factors for the various samples were estimated from the relaxation strengths. The *g*-factor was considerably larger (closer to unity) in the blend than either in the copolymer or homopolymers. This result supports the conclusion reached on the basis of dynamics that the local environment of the blend is heterogeneous at the segmental level.

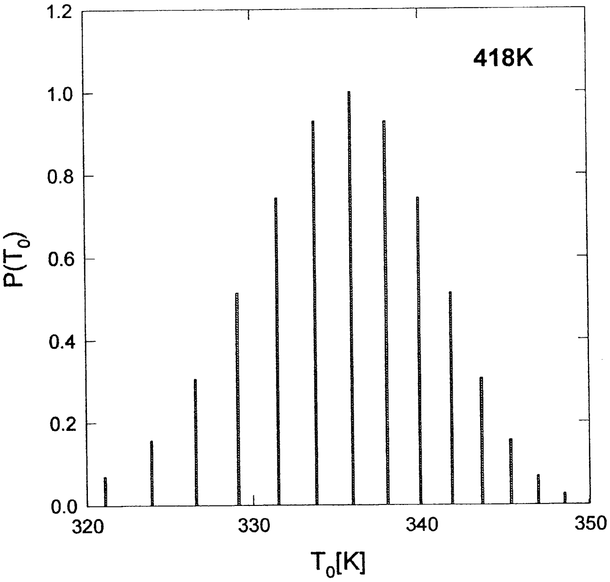

Fig. 13. The distribution, $P(T_0)$, of Vogel–Fulcher temperature, T_0, estimated from $P(T_0)$ by the Vogel–Fulcher equation Eq. (23).

Acknowledgements

The authors thank Prof. R. Koningsveld of University of Leuven for assistance in the calculations of the phase diagram; Prof. G. Williams of the University of Swansea for helpful advice about dielectric measurements and analysis; and Prof. T.K. Kwei of the Polytechnic University for useful discussion about heterogeneity in the polymer blends. One of us (FEK) thank the Air Force Office of Scientific Research for support.

References

[1] Flory PJ. Principles of Polymer Chemistry. Ithaca: Cornell University Press, 1953 (Chap. XIII).

[2] de Gennes PG. Scaling Concepts in Polymer Physics. Ithaca: Cornell University Press, 1979 (Chap. IV).

[3] MacKnight WJ, Karasz FE. Polymer blends. In: Allen GA, Bevington JC, editors. Comprehensive polymer science, vol. 2. Oxford: Pergamon Press, 1989. p. 111–30.

[4] Koningsveld R, Kleintjens LA, Schoffeleers HM. Pure Appl Chem 1974;39:1.

[5] Jeon HS, Lee JH, Balsara NP. Phys Rev Lett 1997;79:3274.

[6] Kwei TK, Nishi T, Roberts RF. Macromolecules 1974;7:667.

[7] Bovey FA, Mirau PA. NMR of polymers. San Diego: Academic Press, 1996 (Chap. IV).

[8] Cimmino S, Karasz FE, MacKnight WJ. J Polym Sci, B: Polym Phys 1992;30:49.

[9] Williams G. Dielectric properties. In: Allen G, Vevington JC, editors. Comprehensive polymer science, vol. 2. Oxford: Pergamon Press, 1989 (Chap. 7).

[10] Runt JP, Fitzgerald JJ, editors. Dielectric spectroscopy of polymeric materials. Washington, DC: American Chemical Society, 1997.

[11] Matsuoka S. Relaxation phenomena in polymers. New York: Hanser, 1992.

[12] Matsuoka S. J Res Natl Inst Stand Technol 1997;102:213.

[13] Shears MF, Williams G. J Chem Soc, Faraday Trans 1973;2(69):609.

[14] Wetton RE, MacKnight WJ, Fried JR, Karasz FE. Macromolecules 1978;11:158.

[15] Colemenero J, Alegria A, Santangelo PG, Ngai KL, Roland CR. Macromolecules 1994;27:407.

[16] Alegria A, Colmenero J, Ngai KL, Roland CM. Macromolecules 1994;27:4486.

[17] Katana G, Fisher EW, Hack Th, Abetz V, Kremer F. Macromolecules 1995;28:2714.

[18] Zetsche A, Fischer EW. Acta Polym 1994;45:168.

[19] Kumar SK, Colby RH, Anastasiadis SH, Fytas G. J Chem Phys 1996;105:3777.

[20] Alexandrovich PS, Karasz FE, MacKnight WJ. J Macromol Sci, Phys B 1980;17:501.

[21] Zacharius SL, ten Brinke G, MacKnight WJ, Karasz FE. Macromolecules 1983;16:381.

[22] Vukovic R, Bogdanic G, Karasz FE, MacKnight WJ. J Phys Chem Ref Data 1999;28(3):851.

[23] Bogdanic G, Vukovic R, Karasz FE, MacKnight WJ. Fluid Phase Equilib 1997;139:277.

[24] Ryan CL. PhD Thesis, University of Massachusetts, 1979.

[25] Vogel H. Phys Z 1921;22:645.

[26] Fulcher GS. Am Chem Soc 1925;8:339.

[27] McCrum NG, Read BE, Williams G. Anelastic and dielectric effects in polymer solids. New York: Dover, 1967.

[28] Havriliak S, Negami S. J Polym Sci 1966;14:99.

[29] Runt JP. Dielectric studies of polymer blends. In: Runt JP, Fitzgerald JJ, editors. Dielectric spectroscopy of polymer materials. Washington, DC: American Chemical Society, 1997. p. 283–302.

[30] Adam G, Gibbs JH. J Chem Phys 1965;43:139.

[31] Doolittle AK. J Appl Phys 1951;22:1471.

[32] Ferry JD. Viscoelastic properties of polymers. New York: Wiley, 1973.

[33] Frohlich H. Theory of dielectrics. 2nd ed. London: Oxford University Press, 1958.

[34] Fried JR. Doctoral thesis, University of Massachusetts, 1976;94.